

4307

UNIVERSITY OF HAWAI'I LIBRARY

LINKAGE ANALYSIS OF THE *tuft* MUTATION

A THESIS SUBMITTED TO THE GRADUATE DIVISION OF THE
UNIVERSITY OF HAWAI'I IN PARTIAL FULFILLMENT
OF THE REQUIREMENTS FOR THE DEGREE OF

MASTER OF SCIENCE

IN

PHYSIOLOGY

August 2008

By

Wallace C. Drumhiller

Thesis Committee:

Dr. Scott Lozanoff, Chair
Dr. Keith S. K. Fong
Dr. Sheri F. T. Fong

We certify that we have read this thesis and that, in our opinion, it is satisfactory in scope and quality as a thesis for the degree of Master of Science in Physiology.

THESIS COMMITTEE



Chairperson

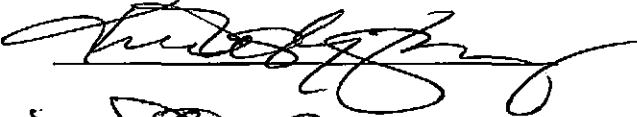




TABLE OF CONTENTS

List of Figures	iv
List of Tables	v
Acknowledgements	vi
Abstract.....	1
Introduction.....	2
Materials and Methods.....	12
Results	24
Discussion	34
Conclusions.....	41
Appendix A.....	42
Appendix B	44
Bibliography.....	46

LIST OF FIGURES

<i>Number</i>	<i>Page</i>
Figure 1	5
Figure 2	7
Figure 3	8
Figure 4	11
Figure 5	14
Figure 6	24
Figure 7	25
Figure 8	26
Figure 9	27
Figure 10	28
Figure 11	29
Figure 12	32

LIST OF TABLES

<i>Number</i>	<i>Page</i>
Table 1	19
Table 2	20
Table 3	21
Table 4	30
Table 5	31
Table 6	33
Table 7	38

ACKNOWLEDGMENTS

The author wishes to express sincere appreciation to Professors Scott Lozanoff and Keith Fong for their assistance in the preparation of this manuscript. In addition, special thanks to Mari Kuroyama, Dr. Ben Fogelgren, and Ms. Tiffany Baring whose familiarity with the procedures, previous and ongoing work was helpful during all phases of this undertaking. Thanks also to the members of the Anatomy and Physiology office for their invaluable support.

ABSTRACT

A spontaneous mouse mutant, *tuft*, exhibits a large intracranial lipoma, the development of which is consistent with a neural tube defect. The purpose of this study was to identify the *tuft* locus, appraise possible candidate genes, and evaluate two different methods of DNA electrophoresis, one of which was used in previous work. Linkage analysis mapped the *tuft* mutation to two candidate regions on chromosome 10 within 16Mb distal and proximal to D10MIT115, at 60Mb and 80Mb respectively. Primers designed by the author for microsatellites in these regions were non informative. A literature survey showed the *tuft* mutation shares a similar phenotype with only one known mutation on chromosome 10 affecting the *Apaf1* gene. A primer designed by the author, WD5, for a microsatellite 2kb from the *Apaf1* gene showed a recombination percentage of 35%. A microsatellite marker within 1cM of the gene containing the *tuft* mutation would be expected to show a near zero recombination percentage. PCR products for two primers designed by the author for microsatellites on chromosome 10 were analyzed using the 4% metaphor gel method, which was previously used, and a Beckman/Coulter CEQ 8000 capillary based method. All samples which showed a result in both methods showed the same result, with a single exception which is likely due to the greater sensitivity of the CEQ. These data suggest that *tuft* maps to chromosome 10 within 16Mb of the microsatellite marker D10MIT115, that the *tuft* mutation is not likely located within the *Apaf1* gene, and that the genotypic methods used are reliable.

INTRODUCTION

Neural tube defects (NTDs) are among the most common birth defects in humans, with reported incidence ranging from about .5 - 6 of every 1000 births^{1,2,3}. The statistics for NTDs vary widely worldwide, but leading variables of incidence appear to be race, geographic region, and sex of the child. Current estimates for the U.S. are between .6 and 1 per 1000 live births, with higher incidence on the east coast and among Hispanic populations^{4,5}. A female predominance of 4:1 has been reported in the U.S.^{6,7,8} An overall drop was noticed from 1991 - 2005 and has been attributed to wider adoption of prenatal screening with subsequent termination of affected pregnancies and folic acid supplements. Folic acid in the maternal diet preceding and during the first weeks of pregnancy has been shown to drop the occurrence and recurrence of NTDs by up to 70%. Despite this environmental factor, a strong genetic component exists, and families predisposed for NTDs have a higher prevalence than seen in the normal population.⁹

Most open NTDs, those where the central nervous system (CNS) is exposed and therefore “open” to an external environment, such as cranioarachischisis where the entire CNS is “open”, are apparent at birth. However, closed NTDs, where the CNS is enclosed, can go undetected for years or decades especially if there are no visible signs, as in some cases of spina bifida. Spina bifida is commonly a closed sacral NTD. The most common NTD compatible with life is myelomeningocele (open spina bifida¹⁰), which occurs in 6000 – 11,000 newborns per year in the United States. Paralysis, bladder and bowel incontinence, and hydrocephalus are the most common clinical complications. Statistics vary, however severe mental retardation is present in about 10-15% of these patients, and about 60% have normal intelligence.¹¹

Recently it was shown that this variation in intelligence is a result of the disease process itself, and not due to complications such as the spinal level of the lesions or existence of a shunt or walking difficulty. Most children with isolated myelomeningocele (without major anomalies of other organs) survive to adulthood, and life expectancy is nearly normal.¹²

NTDs have been shown to have a complex pathogenesis. The long term goal of this project is to help illuminate the pathways and genes responsible for NTDs in the cranial region. To date there are more than 190 mouse mutants and strains which show NTDs¹³. The main thrust of my efforts on the project involve mapping the mutation to a specific chromosome and region, and showing evidence to determine if the *tuft* mouse is a unique murine model for NTD. NTDs are among the most common birth defects in humans, and any model which may help to illuminate the pathways involved would be of substantial value to all future parents as well as investigators hoping to explain, prevent, or eventually treat those affected.

Neurulation

NTDs form due to a defect in the neurulation process. The neural tube forms in humans from the neural plate approximately between stages 9 and 11 on the Carnegie scale (about 19 – 25 days gestation)^{14,15,16}. In mice, this approximately corresponds to stages 11 – 16 of the Theiler scale (formation of neural plate to closure of posterior neuropore)¹⁷.

On about the 20th day of embryogenesis (human) the neural folds close at the 4th somite and proceed in the caudal and cranial direction. The anterior neuropore closes first on about day 26 gestation, and the posterior neuropore follows 2 days later on day 28¹⁸. Since the neuropores close last, most of the NTDs occur at these cranial and caudal locations. The result of a failure of the

cranial neuropore to close commonly results in anencephaly, no brain formation, or exencephaly, brain outside the cranium. Although these two terms are different, they share similar morphology and development since exencephaly is believed to degenerate into anencephaly, a hypothesis supported by animal studies and ultrasonography.^{7,19} Failure of closure of the caudal neuropore commonly results in spina bifida. Failure of closure of either or both neuropores, as the only primary defect, account for ~85% of human NTDs²⁰.

Two processes appear to be involved in the formation of the neural tube: primary neurulation and secondary neurulation (Figure 1). Primary involves the invagination and knitting together of each side of the neural groove, and secondary is canalization. NTDs can be classified as open or closed, based on the presence or absence of exposed neural tissue. Open NTDs frequently involve the entire CNS, and so are often associated with cerebrospinal fluid (CSF) leakage, and are thought to be a result of a defect in primary neurulation. Closed NTDs are thought to be a result of a defect in secondary neurulation, and are often localized to the spine (brain unaffected), and are fully epithelialized. Disturbances to this secondary process can lead to spina bifida or defective development of the cranial vault.¹⁸

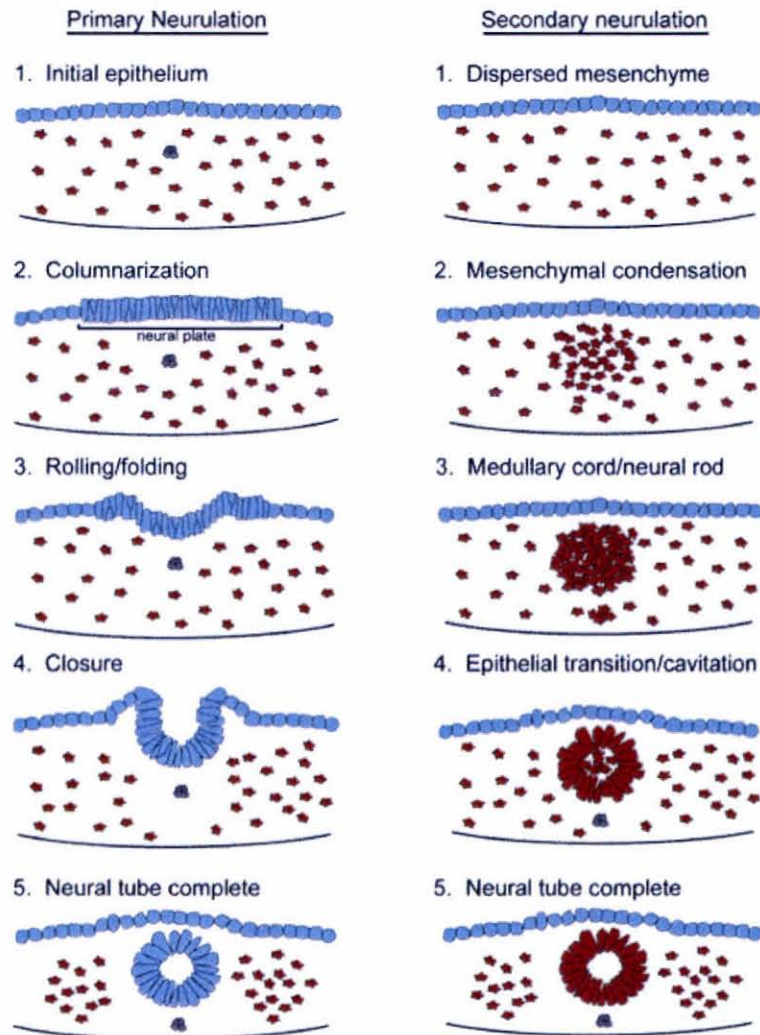


Figure 1 – Comparison of Primary and Secondary Neurulation. Source: http://pharyngula.org/index/weblog/comments/neurulation_in_zebrafish/

Cranial Closure

Closure of the cranial neuropore appears to occur at three distinct locations in the developing murine brain (Figure 2). In the mouse, primary closure of the neural tube is initiated at site Closure 1 at the hindbrain/cervical boundary on embryonic day E8.5 (three weeks post fertilization in humans). Neurulation proceeds in both directions along the future spine. Two more closure points complete the brain formation: site Closure 2 close to the forebrain/midbrain boundary, and site Closure 3 at the rostral end of the forebrain (rostral end of the neural tube/groove).

Closure of sites 1 and 3 seem to be consistent between mouse strains, but there appears to be some variation in Closure 2 among inbred strains²¹ (Figure 3). Strains where site 2 is located closer to the forebrain show an increase in exencephaly, and those where site 2 is located more caudally show less exencephaly²². In fact, a strain called SELH has no site 2 closure point (it is so rostral as to be indistinguishable from site 3) and this strain shows that 1 in 5 embryos develop exencephaly spontaneously²³. This variability in the location of closure site 2 can explain variability in incidence of exencephaly seen between different mouse strains^{24,25}. Humans have been shown not to have a closure site 2, however they do appear to have closure sites equivalent to closure sites 1 and 3²⁶.

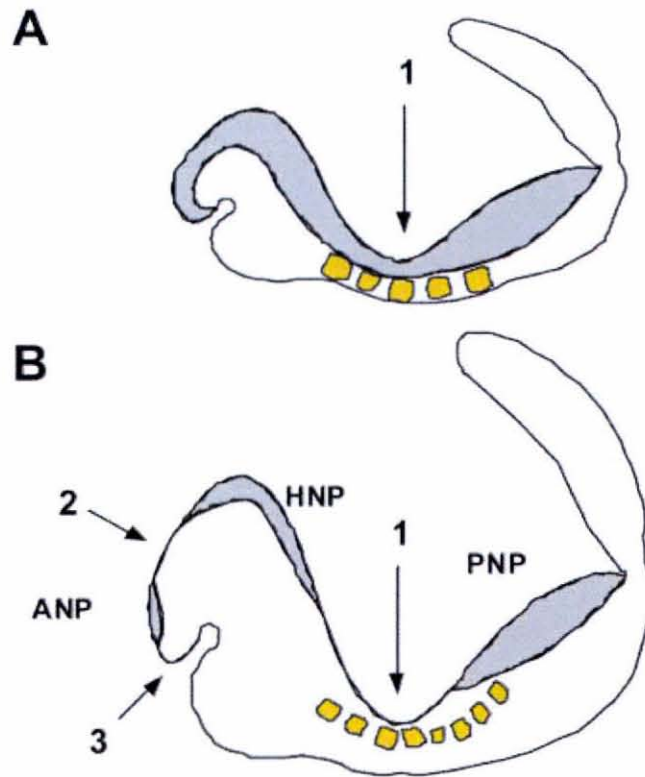


Figure 2 – Locations of closure sites 1, 2, and 3 relative to the developing embryo. The anterior neuropore (ANP), hindbrain neuropore (HNP), and posterior neuropore (PNP) are also labeled on part B. Source: Copp AJ. 2005. Neurulation in the cranial region—normal and abnormal. *J Anat* 207:623–635.

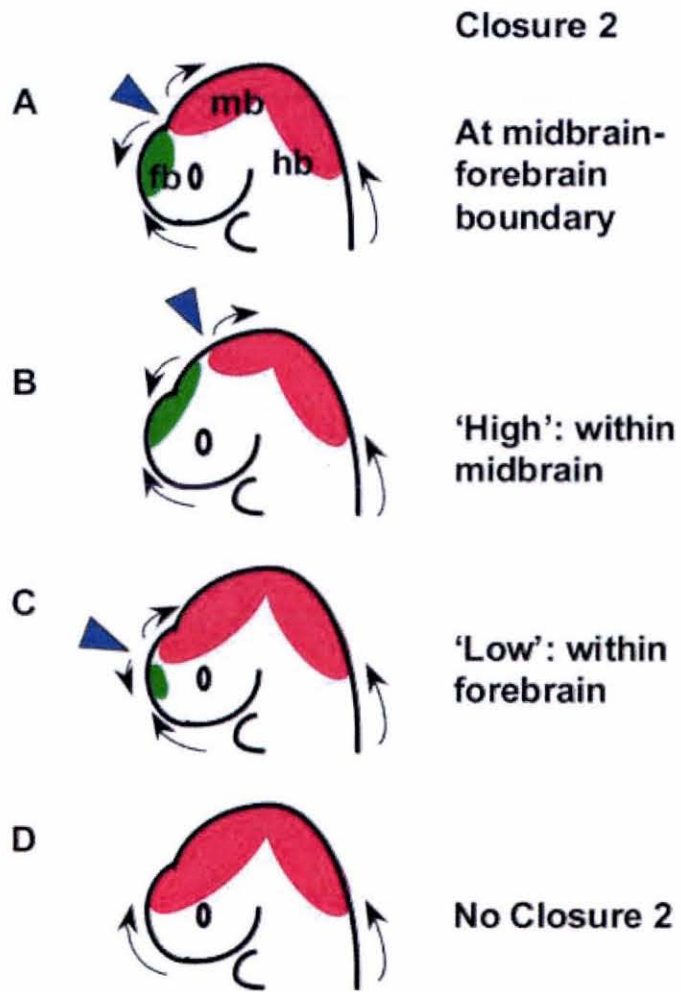


Figure 3 – Sites of Cranial Closure 2. Source: Copp AJ. 2005. Neurulation in the cranial region—normal and abnormal. *J Anat* 207:623–635.

Mouse Models and Current NTD Research

Mice have been used as a model for the study of NTDs for years, and to date there are >80 mutant mouse genes which are known to disrupt neurulation. Although many of the mutants have not been studied in great detail, several crucial pathways for neurulation have been identified. Among these are the planar cell-polarity pathway, which is required to initiate neural tube closure, and the sonic hedgehog signaling pathway which regulates neural plate bending.²⁷ Much of the focus of current NTD research is on folic acid and its role in NTD prevention.

An important question when applying this research to human genetics is whether the genetic risk factors of NTDs are specific to cranial or caudal neuropore closure failures, or if a risk to one is associated with a risk of the other. Of the >190 mouse mutants and strains which show NTDs, 70% have **only** exencephaly and 5% have **only** spina bifida. Of the remainder, 20% can have either or both (spina bifida and exencephaly), and 5% showed cranioarachischisis, where the entire neural tube failed to close²⁸. Overall, the majority of mouse mutants seem to be at risk of neural tube closure failure at only one location (cranial or caudal). The *tuft* mouse appears to be part of the largest group that only shows exencephaly, however a white patch in the sacral region has been observed in a rare few homozygous mice. Further phenotypic analysis is currently ongoing.

Cranial NTDs are more prevalent than caudal NTDs in mice. However, in humans, the number of cranial versus caudal NTDs are close to equal, even within families. It appears 30-50% of families with two affected siblings show one sibling with anencephaly and the other with spina bifida^{1,29,30,31}. The higher number of cranial NTDs in mice versus the seemingly equal number of cranial and caudal NTDs in humans could reflect a difference between species in

embryonic morphology of the cranial neural tube. Neurulation stage human embryos have a proportionately smaller brain than mouse embryos, possibly making elevation of the cranial neural folds easier in the human³².

The *tuft* project centers on a mouse mutation which arose spontaneously in the 3H1 stock mouse population at the University of Hawai'i John A. Burns School of Medicine (Figure 4). This mutation is a promising model for studying neural tube defects. It is characterized by a variable phenotypic expression ranging from a large visible blonde tuft, to a broad skull with associated hypertelorism. MRI of the 3H1 homozygous mutant (*tu/tu*) mouse shows an intracranial lipoma as well as frontal bone agenesis. Staining for cartilage and ossification support these findings, as do results from histological sectioning performed in our lab. The position and growth of the tumor through development are consistent with a neural tube defect. The hypothesis to be tested in this project is that the tuft mutation is located within a specific locus that has not been characterized in the murine genome.



Figure 4 – Unpublished picture of *tuft* mouse courtesy of Dr. Scott Lozanoff 2008. The phenotype of interest is the cranial lipoma.

MATERIALS AND METHODS

Linkage and Recombination

The linkage of a genotype with a phenotype, or genetic linkage, is a direct result of the physical linkage of two or more loci along the same pair of DNA molecules which define a particular set of chromosome homologs in the diploid genome³³. The two linked loci in this project can be defined as the *tuft* mutation and any one of the specified microsatellite markers. In the absence of crossing over between homologs, each gamete of a heterozygous parent receives one or the other of a coupled set of alleles. If there was a crossover between the loci in question, or recombination event, the gamete would receive a non parental combination of alleles. Crossing over occurs randomly along all chromosomes in the genome, therefore the further apart two loci are from each other, the greater chance there is for a crossover. Alternatively, the closer two loci are, the smaller the chance for a chromosome recombination. The frequency of these recombination events can be measured among the samples in a pool and can therefore provide an estimate of genetic distance between the two loci. This project aimed to measure the frequency of recombination between the *tuft* mutation and specific microsatellites, to resolve the location of the *tuft* mutation.

The recombination frequency is reported as a percentage. As the two loci become further apart, or do not share the same chromosome, or as microsatellites are chosen further from the *tuft* mutation, the recombination percentage approaches 50%. Alternatively, if the two linked loci are closer (on the same chromosome), or as microsatellites are chosen closer to the *tuft* mutation, then the recombination percentage approaches 0%. The recombination percentage as an estimate of genetic distance in mice, for this project, uses the following relationship: 1% = 1cM (centimorgan) = 1Mb (million base pairs)³³. For example, if a recombination rate is 20% at a given microsatellite, then the *tuft*

mutation was expected to be within 20 million base pairs of that location on the chromosome (either proximal or distal).

Breeding Strategy

The breeding strategy was in place before the author joined the project, and was largely the work of Dr. Scott Lozanoff and Ms. Tiffany Baring. The mice were selected for breeding based on phenotype, and the genotype was later confirmed in microsatellite analysis. Homozygous mutant inbred 3H1 mice (*tu/tu*) were crossed with Balb inbred mice to create an F1 generation. No mutant phenotype was seen in any F1 mice, so the mutation was considered both non sex linked, and recessive. This F1 generation was considered a carrier of the 3H1 *tuft* mutation, and was mated to the original homozygous 3H1 (*tu/tu*) inbred stock. This backcross N2 generation was expected to contain 50% homozygous (*tu/tu*) mice, and these were expected to contain only 3H1 DNA at the mutation locus. However, due to difficulty in maintaining a steady 3H1 (*tu/tu*) stock population and subsequent sample generation difficulty, an attempt was made to backcross the mutation from the N2 (*tu/tu*) generation onto a Balb background (See Figure 5). The author's efforts in this project focused on narrowing the critical region for the *tuft* mutation by analyzing DNA samples from affected mice of the N2 and greater generations for recombination events.

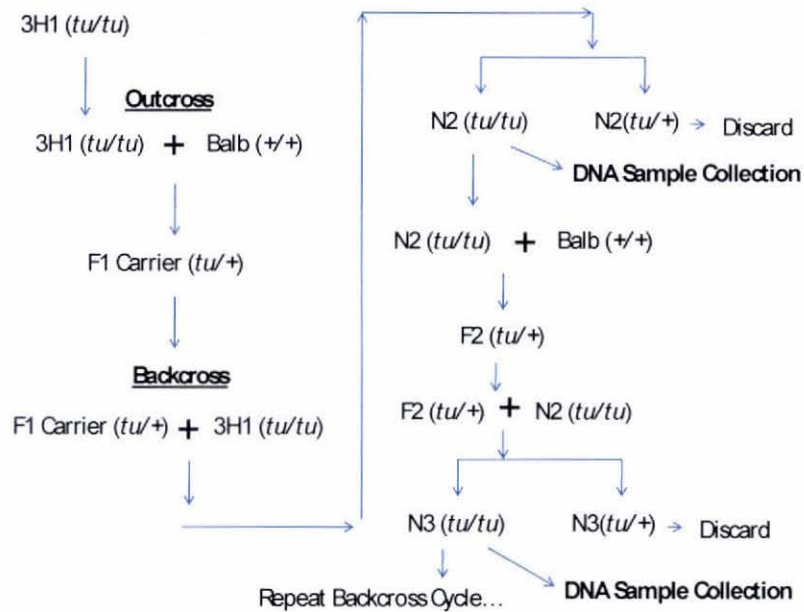


Figure 5 - Breeding Strategy

DNA samples in this project were collected from adults and embryos of the N2 and greater generations. Breeding was based on phenotype followed by testing for genotype. The 3H1 homozygous mutant *tu/tu* stock numbers were difficult to maintain. An attempt was made to backcross the mutation onto a Castaneous background, but had little success. A different attempt to backcross the mutation from the N2 generation onto a Balb background had greater success. These attempts at moving the mutation onto a different background are ongoing at the time of this writing. The success of this effort would result in a more stable stock population and greater selection of informative microsatellite markers.

Two methods were used for DNA analysis, 4% metaphor gel (Lonza) electrophoresis and a Beckman/Coulter CEQ 8000 capillary electrophoresis based machine. A similar approach to score individual samples was used. Bands or peaks corresponding to the 3H1 control only were counted as non-recombinant *tu/tu*. Samples displaying bands or peaks corresponding to both 3H1 and Balb control were counted as recombinant *tu/+*.

DNA Sample Collection

Genomic DNA from adult tissue samples and embryos of affected N2 or greater was collected from tail tissue. Samples were incubated with 700uL of tail buffer with 30uL of 20mg/mL Proteinase K (Ambion), vortexed, and digested overnight at 55°C. The tail buffer consists of: 50mM Tris-Cl at pH8.0, 50mM EDTA, 100mM NaCl, and 1%SDS. The next day the samples were vortexed again, centrifuged at 14,000rpm for 5min, and the supernatant transferred to a new Eppendorf tube. An equal volume of ETOH was added, and the stringy DNA precipitate was transferred to a new tube using a p200 pipette tip with 1mL of 70% ETOH. The DNA was then dried at room temperature, and dissolved in 150-300µL 10mM Tris-Cl, pH 8.5, and stored at 4°C or colder. The author assisted with collection and extraction of the DNA samples, although much of this work was previously performed by Ms. Mari Kuroyama and Ms. Tiffany Baring. At the time of this writing, 82 DNA samples of homozygous mutant (*tu/tu*) mice from the N2 generation had been collected. The author estimates to have assisted in the collection and extraction of at least 10 of those samples.

Primer Design

Once the sample of individual specimens was sufficiently large, microsatellite analysis was utilized to associate the mutation with a single chromosome. Three locations were selected along the length of a given chromosome approximately dividing it into thirds. Three initial locations would allow good coverage of a chromosome without being prohibitive in terms of time or expense. Primers in these locations were either ordered from existing catalogs or were designed by the author. To design the primers, a 200k base pair sequence for each location was downloaded from the Ensemble Genome Database and copied into a word processing program (Microsoft Word). The document was scanned for microsatellite sequences, which are repeated segments of DNA. The sequence CACACACACACACACACA had been used successfully in Dr. Lozanoff's lab, and so was used by the author in this project. The general rule that was used for microsatellite identification was a minimum length of 10 repeats, although more was acceptable as long as the overall length (including primer sequences) was less than 200 base pairs, in order to allow resolution on a 4% metaphor gel (Lonza). Primer sequences on either side of the microsatellite were then chosen.

It is important to note that longer microsatellites are more likely to differ in length between mouse strains. Also, mouse strains that have similar origins, genetically or possibly geographically, are more likely to have similar microsatellite sizes. The goal is to design primers which allow amplification of a microsatellite which has a different length in each of the two mouse strains used in the breeding strategy. Once it is established that a specific microsatellite has a different length in each of the mouse strains, it can then be amplified from each sample in the pool via PCR for further analysis.

Once the microsatellite was located and highlighted in the word processor, primer sequences on each side of the microsatellite were identified using the following guidelines:

- Primer sequences should be 20 – 24 base pairs in length.
- Forward and reverse primers should be same length.
- The ends of the primer sequence should not be the reverse complement of each other. This avoids the amplified section of DNA sticking to itself and forming a “hairpin” shape.
- The total length of the amplified fragment should be as small as possible (start of forward primer to end of reverse primer). The fragment should be approximately 100 – 200 base pairs long, so that small differences are more likely to be revealed on a metaphor gel (Lonza).
- Limit repeats, especially CA or GT.
- Each primer should have only a maximum of 4 of the same base in a row (AAAA, TTTT, GGGG, CCCC).
- The 3' end of each primer sequence should terminate in GC or CG, GG or CC (The 3' end is the end closest to the microsatellite). This is known as a “clamp” because the G-C bond between DNA strands contains three hydrogen bonds, and so it is stronger than the T-A bond which has only two.
- The fragment should maintain a 50/50 ratio of GC to AT bases in each primer sequence.

It is very important to remember, when ordering primers, that the reverse primer must be converted to its reverse complement before ordering, (e.g. CAACG will be CGTTG). In practice it is very difficult, if not impossible, to find a primer sequence which perfectly adheres to all of these guidelines.

Primer Testing

To assess whether a primer pair represents an informative microsatellite, a PCR control set was examined for each primer (3 lanes: water, 3H1, Balb). Optimization was started by using a standard PCR profile and polymerase. Each PCR tube contained 16.25µL RNase – free water (USB corporation), 2.5µL 10x PCR Gold buffer (Applied Biosystems), 2.0µL 25mM MgCl₂ (Applied Biosystems), 0.5 µL 10mM deoxyribonucleotide triphosphate (dNTP), 1.25µL 20µM forward primer, 1.25µL 20µM reverse primer, 0.25µL Amplitaq Gold polymerase (Applied Biosystems). Pairs of oligonucleotide primers were used to amplify each microsatellite marker using Amplitaq Gold polymerase, and a Thermo Electron thermocycler with a PCR profile consisting of an initial denaturation at 94°C for 10min., then 40 cycles of 30 sec. at 94°C (denaturation), 30 sec. at 50 - 58°C (annealing), and 30 sec. at 72°C (extension), with a final extension at 72°C for 4 min.. The PCR products were separated by electrophoresis in a 4% metaphor gel (Lonza) and stained with ethidium bromide. The gels were photographed (Kodak Gel Logic 200) and genotypes were scored informative or non informative.

Metaphor gel can resolve down to 4 base pairs. A primer is scored informative if two bands can be distinguished upon gel electrophoresis, representing different length microsatellites.

Primers Used: Initial Survey

The chromosomes were surveyed sequentially starting with chromosome 1. Ms. Baring and the author worked together on this survey. Microsatellites from chromosomes 1 – 4 were used for the initial scan. An initial screen for possibly informative primers revealed a limited sample (Table 1). In addition, chromosome 10 was selected for analysis, since *tu/tu* shared phenotype similarities with the murine *fog* mutation.

Table 1: Initial Survey Primers

<u>Chromosome 1</u>	<u>Chromosome 2</u>	<u>Chromosome 3</u>	<u>Chromosome 4</u>
D1MIT90*	D2MIT63*	D3MIT158	D4MIT203*
D1MIT58*	D2MIT295*	D3MIT203	D4MIT262*
	D2MIT200		D4MIT12
			D4MIT18

*All primers in Table 1 marked with an asterisk were used by the author. Not all primers in table 1 were informative. All primers in table 1 are catalog primers.

Primers Used: Chromosome 10

A combination of primers synthesized based on sequences from <http://www.informatics.jax.org/> and primers designed in our lab were used for chromosome 10. (Table 2 & Table 3)

Table 2: Catalog Primers Used on Chr. 10

Primer Name	C3H (bp)	Balb (bp)	Location (Mb)
D10MIT238	116	116	20.72
D10MIT115	143	127	69.7
D10MIT230	114	138	89.62
D10MIT134*	93	119	104.01

* The author's assistance was limited with respect to catalog primers without an asterisk. Sizes and map locations indicated on table 2 are from the Jackson.org database, and include the entire amplified product consisting of the microsatellite and primers.

The designed primers used in the project were designed by the author, with guidance by senior lab personnel.

Table 3: Informative Primers Designed by the Author Chr. 10

Primer Name	Primer Sequence	Expected Fragment Size (bp)	Location (Mb)
WD5F	TCTGACATCTACATACATGC	177	90.2
WD5R	TAGGCTGAGAGATGCTAAGC		90.2
TWD2F	CGTTGCTGTGAGGACAATGC	215	48.8
TWD2R	TGGTTCAGAGCCTGGTTTGG		48.8

Many other primers designed by the author were non informative for 3H1 and Balb strains (see appendix B).

Full Sample Run and Scoring

Both WD5 and TWD2 informative microsatellite primers were used in PCR on all DNA samples and PCR products were analyzed using either the CEQ 8000 or 4% metaphor gel (Lonza) method. The PCR profile for samples destined for the CEQ analysis method required D4 labeled forward primers. Final PCR profiles and methods were the same as those discovered to be optimal in the primer testing phase. WD5 Primer optimization required changing the polymerase to Accuprime Taq (Invitrogen), but the TWD2 primer did not require any change from the initial standard PCR profile. WD5 used an annealing temperature of 50°C, and TWD2 used an annealing temperature of 57.3°C. Both pairs of oligonucleotide primers were used to amplify each microsatellite marker using a Thermo Electron thermocycler with a PCR profile consisting of an initial denaturation at 94°C for 10min., then 40 cycles of 30 sec. at 94°C (denaturation), 30 sec. at 50 - 58°C (annealing), and 30 sec. at 72°C (extension), with a final extension at 72°C for 4 min..

The PCR products were separated using two methods. The first method separated PCR products by electrophoresis in a 4% metaphor gel (Lonza) and stained with ethidium bromide. Xylene cyanol (XC) or tricolor loading dye was used (Invitrogen), and the gel remained in the chamber for 60min. at 100V, and 400mA. The gels were photographed (Kodak Gel Logic 200) and genotypes were scored for recombination (See Figure 3).

The second method, the Beckman/Coulter CEQ 8000 is an automated machine using capillary electrophoresis for DNA fragment separation. In order for the PCR product to be detected by the machine, it must fluoresce following laser excitation. This is accomplished by using special D4 labeled forward primers

in the PCR step. The primer sequences for the CEQ are the same as those used in the gel method.

To perform a run on the CEQ 8000, a 0.5uL aliquot of the D4 labeled PCR product was placed into each well on a sample plate followed by 0.5uL of standards mix (Beckman), and 39uL of sample loading solution (Beckman). The capillary array, gel cartridge, buffer plate, and sample plate were then loaded into the machine (all available from Beckman), and the samples were run using either of the standard fragment test methods highlighted in the software menu, FRAG3 or FRAG4. The output is a series of peaks, which correspond to known fragment sizes. Scoring CEQ data consists of comparing the sample peaks to control peaks. A sample with a single peak corresponding to the 3H1 control was scores as homozygous *tu/tu*. A sample containing two peaks corresponding to both 3H1 and Balb control peaks was scored as a recombinant heterozygous *tu/+*.

In both methods the total number of recombinants was divided by the total number of non-recombinants, multiplied by 100 to determine a percentage. A comparison of individual sample scores and recombination percentages was conducted to determine the reliability of data collected by both methods.

RESULTS

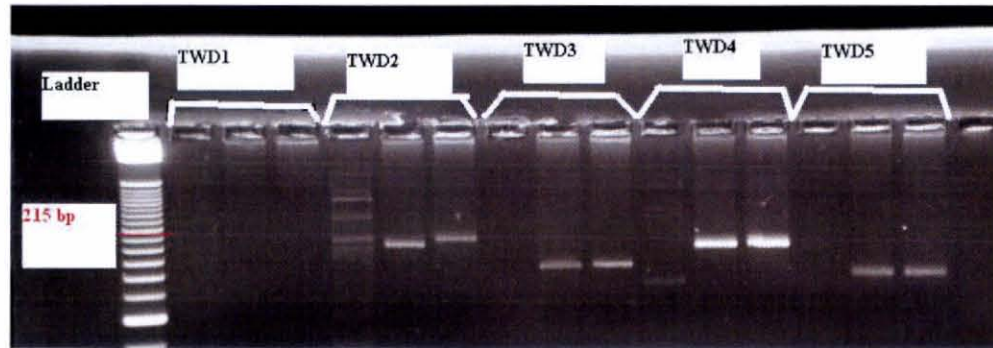


Figure 6 - Amplimers of TWD series primer testing. The first lane (far left) is a 25 base pair ladder. Each group of 3 lanes as indicated by the primer sets TWD 1 – 5 contains PCR products from left to right: water, 3H1 genomic DNA, Balb genomic DNA.

An example of how primers were determined to be informative for analysis is shown in Figure 6. The expected fragment size for TWD2 was 215 base pairs (bp). TWD1 shows no PCR amplification and groups TWD3-5 were also not informative because we could not distinguish the lengths of the amplified products from 3H1 and Balb DNA. TWD2 alone was informative because the predicted fragment size of 200 bp was amplified from 3H1 DNA, while a size of about 215bp was amplified from Balb DNA. Although bands were detected in the water negative control for TWD2, they were not intense nor replicated in any of the other lanes. Only 3 primer pairs out of 24 pairs tested were informative (TWD2, WD4, and WD5).

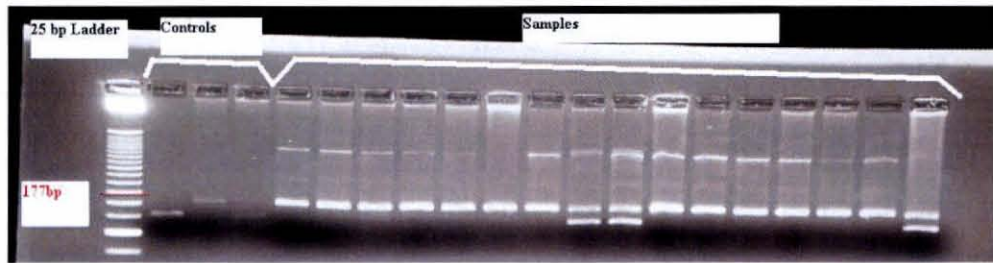


Figure 7 - Gel 1 from the full run of the WD5 primer. The first lane (far left) is a 25 base pair ladder. The control lanes contain PCR products from left to right: water, 3H1 genomic DNA, Balb genomic DNA.

An example of a gel from a full run is shown in Figure 7. Although a band was detected in the water negative control with a product similar in size to the Balb control, it is clearly not replicated in any of those samples scored as non-recombinant homozygous. The expected fragment size was 177bp. This gel shows three recombinant heterozygous (*tu/+*) samples in lanes 12, 13, and 20.

balb control.A01_08041223SO

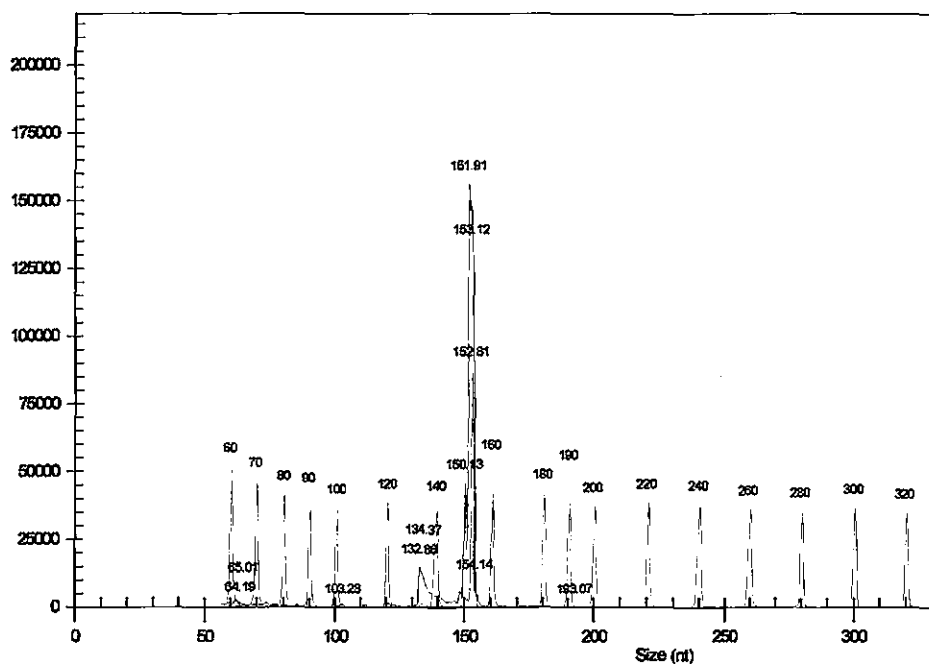


Figure 8 - CEQ output of the Balb control from the WD5 full run.

An example of a Balb control on the CEQ is shown in Figure 8. The CEQ software determined the fragment size of the control peak by comparing it to the known fragment sizes of the standard mix, shown as red peaks. For scoring purposes, the highest peak identified by the software was used. The fragment size of the Balb control represents the total fragment size of the PCR product, including the microsatellite, and is shown in a peak here corresponding to a size of 151bp. The expected fragment size for WD5 was 177bp.

3h1 control.B01_08041223SN

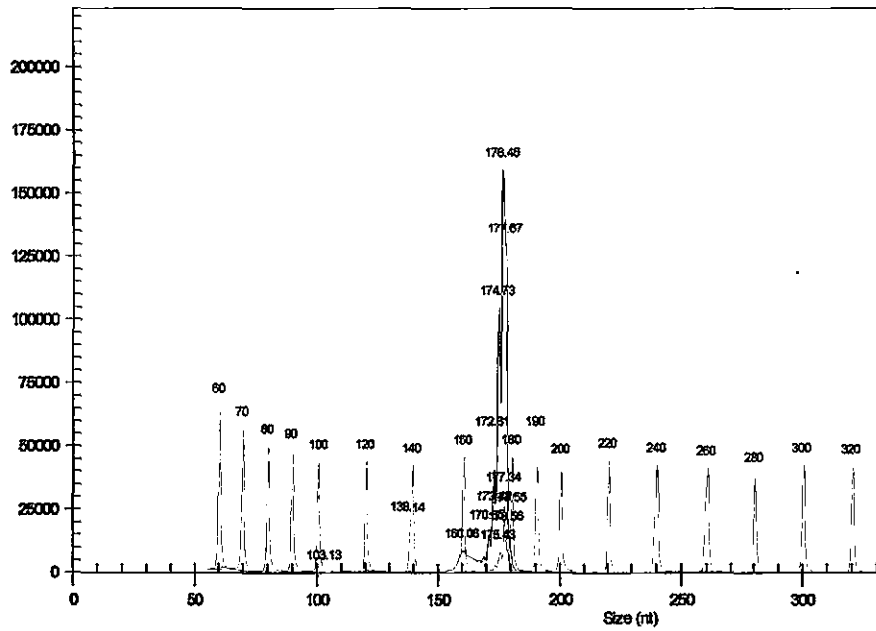


Figure 9 - CEQ output of the 3H1 control from the WD5 full run.

An example of a 3H1 control from the CEQ is shown in Figure 9. The expected fragment size for WD5 was 177bp. The peak corresponds to 176bp, and so is very close to the expected fragment size.

45.D06_08041223RD

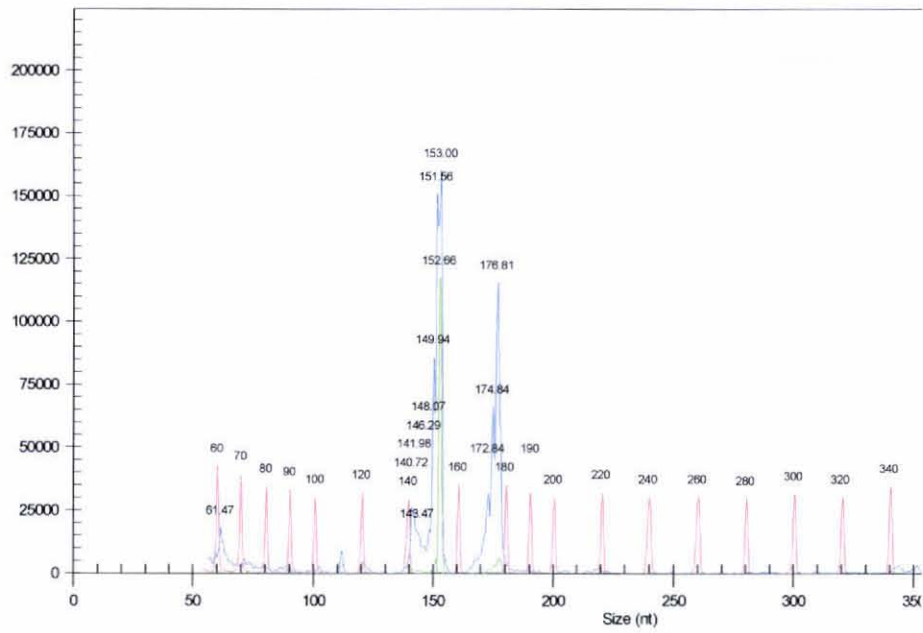


Figure 11 - CEQ output of sample 45 scored as heterozygous from the WD5 full run.

An example of a heterozygous sample scored as recombinant *tu/+* from the WD5 full run is in figure 11. This is sample 45, and it shows two peaks which correspond to the Balb and 3H1 controls at 151bp and 176bp respectively. A recombination event occurred between the *tuft* locus and the WD5 microsatellite on this sample.

Table 4 – Initial survey results showing recombination percentages for chromosomes 2 through 4

Chromosome	Primer	Recombination %
1	NONE	NONE
2	D2Mit200	53%
3	D3Mit158	56%
4	D4Mit18	48%

The initial survey of chromosomes 1 – 4 were run using the 4% metaphor gel method and showed recombination percentages around 50%. This demonstrates no linkage between the *tuff* locus and these markers. It is possible that the *tuff* locus is more than 50Mb away from these markers on the same chromosome. However, because the screening from chromosome 10 markers showed a positive LOD score, it was reasonable to exclude chromosomes 2 – 4. No informative primers were found for use on chromosome 1. These results support the idea that the *tuff* mutation is not located on chromosomes 2 – 4.

**Table 5 – Experimental and statistical results for chromosome 10
calculated by Map Manager software.**

Marker	X	N	Distance (cM)	LOD
WD5	27	70	38.6	0.8
D10MIT283	22	73	30.1	2.6
TWD2	15	73	20.5	5.9
D10MIT115	10	61	16.4	6.5
D10MIT230	22	70	31.4	2.1
D10MIT134	27	67	40.3	0.6

Results based on data using gel method. This table was computed using Map Manager software found at www.mapmanager.org³⁴. For comparison between gel and CEQ methods, see Table 6. The column X represents the number of recombinants corresponding to the microsatellite, while column N shows the number of samples for each microsatellite. The remaining columns show the distance, in centiMorgans, the microsatellite is estimated from the site of the *tuft* mutation, and the LOD score. The LOD score is a statistical test, reported as a logarithm base 10, used in linkage analysis to determine linkage between a trait and a marker. By convention, and LOD score greater than 3 is considered evidence for linkage. The markers TWD2 and D10MIT115 showed linkage to the *tuft* mutation.

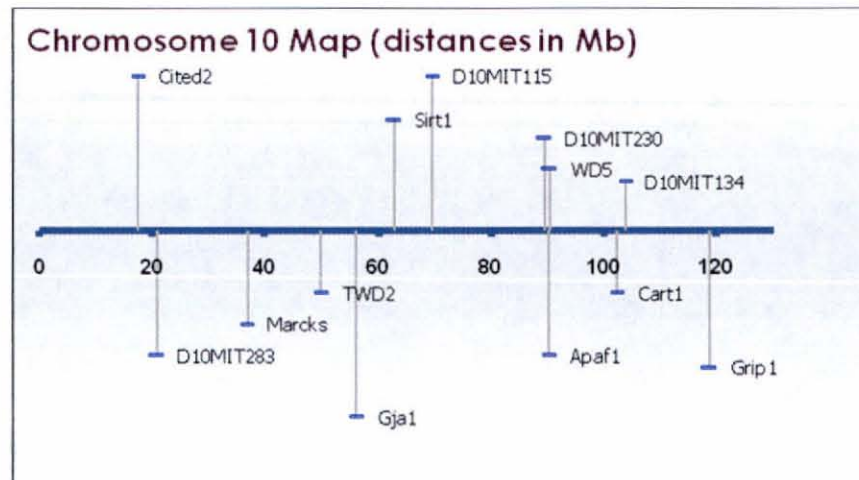


Figure 12 – Map of Chromosome 10 containing all markers and candidate genes.

All of the candidate genes discovered in the literature survey as well as the informative microsatellite markers used on chromosome 10 are displayed relative to each other in Figure 11. See Table 7 in the discussion section for analysis of the candidate genes.

Table 6 – Comparison of the recombination percentages from the CEQ and gel methods.

Primer Site	Method	Recombination Percent Score
TWD2 (49.98Mb)	GEL	15/81 = 18.5%
TWD2 (49.98Mb)	CEQ	13/77 = 16.8%
WD5 (90.52Mb)	GEL	27/77 = 35%
WD5 (90.52Mb)	CEQ	28/77 = 36%

The recombination percentages were very similar between the methods used. A few of the samples using the gel method did not amplify on the first PCR attempt. Although some of these samples did eventually amplify, a few did not and therefore were not used in the calculation. Some of the samples using the CEQ method had similar trouble, and did not generate identifiable peaks due to salt or sample concentration being too high. Dilution was able to resolve some of these samples, but not others. Of the samples which gave results in both methods, all were identical except a single sample in the WD5 run. This sample scored as homozygous Balb using the gel method, and as heterozygous (*tu/+*) using the CEQ. This is likely explained by the higher sensitivity of the CEQ method, that a band was not visible using the gel method. This data supports the idea that both methods are reliable, and generate repeatable results.

DISCUSSION

The initial phase of this project was to genotype mice from backcrosses which demonstrated the *tuft* phenotype. A total of 82 DNA samples from homozygous *tuft* mice were collected. This study analyzed two microsatellites, TWD2 and WD5, using both the 4% Metaphor gel and Beckman/Coulter CEQ 8000 methods, in order to further narrow down the *tuft* locus and verify previous electrophoresis methods. A small number of samples showed a single band or peak corresponding to the Balb control. This was unexpected, because all of the samples came from affected mice with a 3H1 background, so all samples should show at least one band corresponding to the 3H1 control. The most likely explanation is that some of the (*tu/tu*) samples were collected from an attempt to back cross the *tuft* mutation onto a Balb background. The N2 generation was repeatedly backcrossed with Balb inbred strain, and some of the samples may have come from the later second or third generation backcrosses. This would introduce more Balb DNA, and each generation would increase the possibility of a microsatellite testing as homozygous Balb. This is likely the case, and would not greatly affect the recombination percentages that were calculated, since those samples which tested Balb were few and were not included in the calculation.

The 3H1 strain came from a mating of C3H and H101. C3H came from Balb. This connection of 3H1 and Balb strains may explain why it was difficult to find informative primers. An attempt was made to backcross the mutation onto a Cast background, but has yet been unsuccessful. Greater success has been encountered trying to backcross the mutation onto a Balb background.

The small difference of about 2% in recombination percentage seen between the two methods of electrophoresis appear to be completely due to a few samples not showing results. In the gel method, this is due to non-detectable amplification on the PCR step. On the CEQ this is due mostly to the peak

intensity being too high which is a result of PCR product and salt concentration in the sample well being too high. The samples which gave results in both methods were completely identical, with the exception of a single sample in the WD5 series. This sample showed as a Balb using the 4% metaphor gel method, and as a *tn/+* using the CEQ. The CEQ is much more sensitive than the 4% metaphor gel method, so it is possible that it was able to resolve a band that was too faint to see in the gel picture. The author feels that the data produced using either method is reliable based on these results.

The advantages and disadvantages of using the CEQ versus gel method are fairly straightforward. The CEQ requires less work overall, since the actual run is automated. The only work required is in sample preparation, array and gel cartridge insertion, and software setup. The run time for the CEQ is about 90 minutes per row of 8 wells. Also, as mentioned before, the CEQ is much more sensitive, and can resolve individual base pairs. One significant advantage of the CEQ method is that the samples in the tray can be covered and stored and run again when needed. The length of storage is entirely determined by the shelf life of the D4 primer used in the samples. Beckman literature says these primers have a shelf life of about a year when stored dry at -20C.³⁵ The CEQ uses specialized D4 labeled primers which are significantly more expensive than standard primers used in the gel method (\$200 per pair vs. \$8 per pair via Integrated DNA Technologies, IDT). The gel method requires more work since the gels need to be made, dye added to PCR product, wells loaded, and gels photographed upon completion. The speed of this process is entirely dependent on the familiarity of the technician with the protocol, the number of gels able to be run at a time, and the number of samples needed to be run. The author only had equipment to run 2 gels at a time and used a single row of 20 wells on a 4% metaphor gel.

Essentially the CEQ is more sensitive and can resolve single base pair differences, requires less work on the part of the operator, but is significantly more expensive, especially on smaller sample sizes. The gel method is cheaper, especially on smaller sample sizes, but requires more work on the part of the user. It is therefore the opinion of the author that the gel method should be used to analyze primers and on small sample pools, and the CEQ should be employed using informative primers on large sample sizes.

The Beckman/Coulter CEQ 8000 has been used in other similar gene mapping studies. One involved mapping a malaria vector³⁶, while another involved comparative mapping of bovine chromosome 27³⁷. The Beckman literature even suggests using the CEQ 8000 for studying single nucleotide polymorphisms³⁸. It is worth noting that using the CEQ 8000 on a mapping project such as the *tuft* project is not unusual.

Since the gel method was used to determine informative primers, and is only capable of resolving down to 4 base pair differences, it is possible that some of the non informative markers would be informative if the CEQ method were used. However, this would be both time consuming and expensive considering the high cost of ordering the expensive CEQ primers in addition to the gel primers.

The author conducted literature surveys to try and match the *tuft* phenotype with other known mouse mutations without success. The search used three main criteria to screen candidate strains and mutations: exencephaly, able to live past gestation day 12, and have a mutation on chromosome 10. The main sources involved the Jackson Laboratory database³⁹, and Juriloff et al.(2007)²⁸, that when combined contained the most current list of NTD mouse models and strains. Only 8 mouse strains emerged as a result of this search.

Each of the 8 strains on the list had a known gene and phenotype, and most had a known protein function for the gene in question. A table was created containing the 8 strains, the protein function, and any phenotype not shared with the *tuft* mouse as evidence against the *tuft* mutation affecting the same gene as a known mutant strain (Table 7). Only one mutant strain stood out using this method, the *fog* mutant, known to affect the *Apaf1* gene^{40, 41}. The *fog* mutant and the *tuft* mouse share a similar phenotype, and are so close morphologically that differentiation is difficult. Although the *tuft* and *fog* mice share a similar phenotype, the *fog* mouse is known to exhibit webbed toes, curly tails, and spina bifida, along with exencephaly⁴². The *tuft* mouse has been known to exhibit only exencephaly, although a rare white spot in the sacral region has been reported. The *fog* mice that live to adulthood with exencephaly very closely resemble *tuft* mice in appearance. It was for this reason that the WD5 primers were designed around a microsatellite within 2kbp of the *Apaf1* gene. A high recombination percentage at this site would exclude *Apaf1* as a *tuft* candidate gene. A recombination percentage of 35% was found, supporting the idea that the *tuft* mutation does not lie in close proximity to the *Apaf1* gene. However, the similarity in phenotype between *fog* and *tuft* mutations suggests that the same pathway may be involved.

Table 7: Mutant Search

Gene Name	Location (Mb)	Protein Function	Evidence against
<i>Apaf1</i> (<i>fog</i> mutant and null)	90.45	Apoptosis	Linkage analysis showed high % at gene location
<i>Cart1</i>	102.47	Transcription	acrania/meroanencephaly
<i>Cited2</i>	17.44	Transcription	Heart, adrenal, cranial Ganglia also affected
<i>Gja1</i>	56.09	Cell-cell Interaction	Die by GD 14; heart also affected
<i>Grip1</i>	118.89	Cell-matrix Interaction	Spina bifida also, with Eye defects in all non-EX
<i>Marcks</i>	36.85	Actin function	20% omphalocele; 30% runted; corpus callosum, brain, retina affected
<i>Sirt1</i>	62.78	Chromatin	Heart, eye affected
10 (ENU)	Unknown	Unkown	Polydactyly; eye, Cardiovascular system affected; die by GD 13

The high recombination percentage at the WD5 location near the *Apaf1* gene, and the elimination of other known mutant phenotypes affecting chromosome 10, together suggest that the *tuff* mutation is unique. The questions that arise now are: where on chromosome 10 is the *tuff* mutation located, and what gene is affected. An analysis of recombination percentages for all 6 microsatellite locations on chromosome 10 suggest that the most likely locations for the mutation are either around 60Mb, or 80Mb. Primers were designed for both locations, but were found to be non informative. These primer sequences can be found in appendix B. There are a huge number of genes around the regions specified, and even so it is possible that the *tuff* mutation lies on a gene

that has not yet been identified. Some genes from these regions have been reviewed, but no strong candidates have emerged. Since the *fog* and *tuft* mice share such a similar phenotype, the author feels it is reasonable to conclude that the *tuft* mutation may affect a gene which may help regulate expression of *Apaf1*. The *Apaf1* gene codes for a protein which acts as the structural core for apoptosome formation, and is down regulated in the homozygous mutant *fog* mouse. When the mitochondrial apoptotic pathway is activated, cytochrome c is released from the mitochondria into the cytosol and binds to *Apaf1* CARD domain causing a conformational change, followed by a second conformational change by attaching ATP molecules. Seven of these *Apaf1* complexes combine with seven Caspase-9 initiator molecules to form an apoptosome. The apoptosome then functions to activate other caspases and interact with proteins leading to apoptosis⁴³. Down regulation of *Apaf1* during development of the forebrain in the *fog* mouse leads to excess founder-cell populations which leads to exencephaly⁴². If the *tuft* mutation affects a protein which helps regulate *Apaf1*, an experiment which measures the expression of *Apaf1* in the *tuft* mouse should show a difference from the expression found in the 3H1 background. If a difference is seen then attention could be focused on factors known to affect *Apaf1*. If no differences were found, then it could support the idea that *tuft* is unique. More informative microsatellites need to be found in the 60Mb and 80Mb regions of chromosome 10, and run on the full pool of samples in order to both narrow down the location of the mutation and shorten the list of possible candidate genes.

The next steps in this project include locating additional markers around D10MIT115, either by using the higher resolution CEQ method on previously non informative primers, or designing and testing new primers designed around microsatellites in the target regions 16Mb proximal and distal to D10MIT115. Also, other candidate genes should be identified from these target regions, and

screened using linkage analysis. One method for identifying these candidate genes would be to look for genes in the target regions known to affect or regulate the *Apaf1* gene.

CONCLUSION

The recombination percentages for the TWD2 and D10MIT115 primers are much less than 50% (20.5 and 16.4 cM respectively), and the results for the TWD2 primer were reproduced using the CEQ method. This supports the idea that chromosome 10 is the chromosome which contains the *tusft* mutation.

The recombination percentage score for the WD5 primer is much higher than 0% (38.6cM), which supports the idea that the *tusft* mutation does not lie near the *Apaf1* gene. This supports the ideas that the *tusft* mutation is not the same as the *fog* mutation, and that the *tusft* mutation is unique.

APPENDIX A: CATALOG PRIMER LIST

Working Primers:

Chromosome	Distinguish 3H1 and Balb
1	
2	D2Mit200, D2Mit63
3	D3Mit158, D3Mit203
4	D4Mit54, D4Mit18, D4Mit190
5	D5Mit346
6	D6Mit366, D6Mit373, D6Mit116
7	D7Mit152, D7Mit362
8	D8Mit238, D8Mit155
9	D9Mit105
10	D10Mit134, D10Mit283
11	D11Mit288, D11Mit338
12	D12Mit150, D12Mit52
13	D13Mit211
14	D14Mit99
15	D15Mit138
16	D16Mit34, D16Mit63, D16Mit152
17	D17Mit113
18	D18Mit51
19	D19Mit128
X	

Appendix A: Continued

Non working Primers:

Chromosome	Failed to Distinguish 3H1 and Balb
1	D1Mit58, D1Mit90, D1Mit362
2	D2Mit295
3	D3Mit258
4	D4Mit203
5	D5Mit292
6	
7	D7Mit96
8	D8Mit14
9	D9Mit238, D9Mit224
10	D10Mit96
11	
12	D12Mit81
13	D13Mit97, D13Mit167
14	D14Mit107, D14Mit39
15	D15Mit246, D15Mit29
16	
17	D17Mit215
18	D18Mit22
19	D19Mit33, D19Mit13
X	DXMit67, DXMit31

Appendix B: Primers Designed by the Author

Primer Name	Primer Sequence	Primer Location (Mb)	Informative (3H1/Balb)
TWD1F	CTCTACTATAGCAGATTGGC	48.98	UNKNOWN
TWD1R	GTTAATTTAGTTCCTGTGTC	48.98	UNKNOWN
TWD3F	CTAGCTGCAGAGTATCCAGC	48.98	NO
TWD3R	GTCAAATGGTGAGTAATTGC	48.98	NO
TWD4F	CAGTGTTGACTTGGAAATGC	48.98	NO
TWD4R	CTCATGCTTGCGAAGCATGC	48.98	NO
TWD5F	TGAAGAATAAGAAGACACGC	48.98	NO
TWD5R	TTCCCTCTTGACTCTTCTGC	48.98	NO
TWD6F	GACAAGGATTTCAAAC TAGC	48.98	NO
TWD6R	TCTTCAGTGATTCTATCACG	48.98	NO
TWD7F	TCCTACAGCCC ACTAGAAGC	48.98	NO
TWD7R	CACACAATGGGCTCATTGGC	48.98	NO
TWD8F	TAACACAGGTAAACAAGTGG	48.98	NO
TWD8R	CCTTCATCTGTTTGGTTGTG	48.98	NO
TWD9F	TGATGGATACTATCAGGAGC	48.98	NO
TWD9R	GTA AATTCTGTAGGGTGCTC	48.98	NO
TWD10F	GTCTGATCTAGGCGGACAGC	48.98	NO
TWD10R	CCA ACTCCAGGTATTATTGC	48.98	NO
WD1F	TCTGACTCCACATGCATGC	90.52	NO
WD1R	CTCCAGAGCTAAGGGCCAGC	90.52	NO
WD2F	GCTAAGGGACTGCCTTATGC	90.52	NO
WD2R	ATCCATAGTTTAGAGGTACG	90.52	NO
WD4F	AGGAAGGATAGCCAAGTTGC	90.52	YES
WD4R	TATTGAGTCTTCATACATGC	90.52	YES
WD6F	TGTTTGTGCGTACACACACG	90.52	NO
WD6R	CACTGAGCCATCTCACCAGC	90.52	NO
WD7F	GCATGTGCATGCGAGGAACA	90.52	NO
WD7R	GGCTTTGGTTT CACGTTTGC	90.52	NO
WD8F	GCATCCACATCGGGTAGCTC	90.52	NO
WD8R	CCGAGTCTTGGGAAATATTC	90.52	NO
WD11F	CCAGATCCTCCACCACTTCC	59	NO
WD11R	TGTACAGGTCCCATGCTTGG	59	NO
WD12F	CTTCTCTACCTCCAGTTAGC	59	NO

Appendix B: Continued

Primer Name	Primer Sequence	Primer Location (Mb)	Informative (3H1/Balb)
WD12R	TAGATGAGGGTACTCTGTGC	59	NO
WD13F	TCTCCTCCATGCTTTGGCTC	59	NO
WD13R	TGTTTGTGGTGGTGGTAAGG	59	NO
WD14F	CACTGTCTTCTGCCTCAGCC	59	NO
WD14R	GCCCCAAAGGAATATGCTTGG	59	NO
WD15F	ACCATTGAGCTAGTCAAGGC	79	NO
WD15R	GGCTAATCAGGACTTCATGG	79	NO
WD16F	GCAGAGCATGAGGACTGAGC	79	NO
WD16R	CTCCCTTATCTCCATGTCCC	79	NO
WD17F	CTCCAGCACTGGTGCATGC	79	NO
WD17R	GCAGGGAAACTGAGGTGTGC	79	NO
WD18F	TGAGTTCTAGGACAGCCAGG	79	NO
WD18R	CCTAAAGCCGCAGTCCAACC	79	NO
WD19F	GGACCGAAGGAGAGAACTGG	59	NO
WD19R	TCAGCAGCTAGCATGGGAGG	59	NO
WD20F	ACAGGTGTCTTATGAACTCC	59	NO
WD20R	CCAGCATCGTCACCAAGGAC	59	NO
WD21F	ACCCCATGGCATCTCAGAGC	59	NO
WD21R	CTCCTCTGAGGTGTACTAGG	59	NO
WD22F	GTGGTCACACCTGGAATTGC	59	NO
WD22R	TTATACTAGAAATCCTGCGC	59	NO

BIBLIOGRAPHY

¹McBride, M. L. (1979). "Sib risk of anencephaly and spina bifida in British Columbia." Am J Med Genet 3(4): 377-87.

²McGahan JP, Pilu G, Nyberg DA. Neural tube defects and the spine. In: Nyberg DA, McGahan JP, Pretorius DH, Pilu G, eds. *Diagnostic Imaging of Fetal Anomalies*. Philadelphia: Lippincott Williams & Wilkins, 2003:291-334.

³Czeizel, A. E. and I. Dudas (1992). "Prevention of the first occurrence of neural-tube defects by periconceptional vitamin supplementation." N Engl J Med 327(26): 1832-5.

⁴Harris, J. A. and G. M. Shaw (1995). "Neural tube defects--why are rates high among populations of Mexican descent?" Environ Health Perspect 103 Suppl 6: 163-4.

⁵http://www.cdc.gov/nchs/products/pubs/pubd/hestats/spine_anen.htm

⁶Romero R, Pilu G, Jeanty P, et al. (1988) *Prenatal Diagnosis of Congenital Anomalies*. Appleton & Lange, Norwalk. p43-5.

⁷Nyberg DA, Mahony BS, Pretorius DH. (1990) *Diagnostic Ultrasound of Fetal Anomalies: Text and Atlas*. Mosby Year Book, St. Louis. p149-52.

⁸<http://www.obgyn.net/ultrasound/ultrasound.asp?page=/ultrasound/cotm/0006/Exe-ncephaly-Anencephaly>

⁹Beaudin, A. E. and P. J. Stover (2007). "Folate-mediated one-carbon metabolism and neural tube defects: balancing genome synthesis and gene expression." Birth Defects Res C Embryo Today 81(3): 183-203.

¹⁰<http://www.nlm.nih.gov/medlineplus/ency/article/001558.htm>

¹¹<http://www.emedicine.com/NEURO/topic244.htm>

¹²Nejat, F., S. S. Kazmi, et al. (2007). "Intelligence quotient in children with meningomyeloceles: a case-control study." J Neurosurg 106(2 Suppl): 106-10.

¹³Harris, M. J. and D. M. Juriloff (2007). "Mouse mutants with neural tube closure defects and their role in understanding human neural tube defects." *Birth Defects Res A Clin Mol Teratol* 79(3): 187-210.

¹⁴<http://www.emedicine.com/NEURO/topic244.htm>

¹⁵Abd El Ghani, E. A. K. (2006). "Neural Tube Defects." *ASIOG* volume 3(February 2006).

¹⁶<http://www.visembryo.com/baby/9.html>

¹⁷<http://genex.hgu.mrc.ac.uk/Databases/Anatomy/MAstaging.shtml>

¹⁸Gos, M. and A. Szpecht-Potocka (2002). "Genetic basis of neural tube defects. I. Regulatory genes for the neurulation process." *J Appl Genet* 43(3): 343-50.

¹⁹Timor-Tritsch, I. E., E. Greenebaum, et al. (1996). "Exencephaly-anencephaly sequence: proof by ultrasound imaging and amniotic fluid cytology." *J Matern Fetal Med* 5(4): 182-5.

²⁰Hall, J. G., J. M. Friedman, et al. (1988). "Clinical, genetic, and epidemiological factors in neural tube defects." *Am J Hum Genet* 43(6): 827-37.

²¹Juriloff, D. M., M. J. Harris, et al. (1991). "Normal mouse strains differ in the site of initiation of closure of the cranial neural tube." *Teratology* 44(2): 225-33.

²²Fleming, A. and A. J. Copp (2000). "A genetic risk factor for mouse neural tube defects: defining the embryonic basis." *Hum Mol Genet* 9(4): 575-81.

²³Macdonald, K. B., D. M. Juriloff, et al. (1989). "Developmental study of neural tube closure in a mouse stock with a high incidence of exencephaly." *Teratology* 39(2): 195-213.

²⁴Austin, W. L., M. Wind, et al. (1982). "Differences in the toxicity and teratogenicity of cytochalasins D and E in various mouse strains." *Teratology* 25(1): 11-8.

²⁵Finnell, R. H., S. P. Moon, et al. (1986). "Strain differences in heat-induced neural tube defects in mice." *Teratology* 33(2): 247-52.

²⁶O'Rahilly, R. and F. Muller (2002). "The two sites of fusion of the neural folds and the two neuropores in the human embryo." *Teratology* 65(4): 162-70.

²⁷Copp, A. J., N. D. Greene, et al. (2003). "The genetic basis of mammalian neurulation." Nat Rev Genet 4(10): 784-93.

²⁸Harris, M. J. and D. M. Juriloff (2007). "Mouse mutants with neural tube closure defects and their role in understanding human neural tube defects." Birth Defects Res A Clin Mol Teratol 79(3): 187-210.

²⁹Czeizel, A. and J. Metneki (1984). "Recurrence risk after neural tube defects in a genetic counselling clinic." J Med Genet 21(6): 413-6.

³⁰Keena, B., A. D. Sadovnick, et al. (1986). "Risks to sibs of probands with neural tube defects: data for clinic populations in British Columbia." Am J Med Genet 25(3): 563-73.

³¹Drainer, E., H. M. May, et al. (1991). "Do familial neural tube defects breed true?" J Med Genet 28(9): 605-8.

³²Copp, A. J. (2005). "Neurulation in the cranial region--normal and abnormal." J Anat 207(5): 623-35.

³³Lee M. Silver, Mouse Genetics, Oxford University Press, 2005
<http://www.informatics.jax.org/silver>

³⁴Manly, K. F., R. H. Cudmore, Jr., et al. (2001). "Map Manager QTX, cross-platform software for genetic mapping." Mamm Genome 12(12): 930-2.

³⁵Beckman/Coulter 390018-AA, Dye-labeled Phosphoramidites Frequently Asked Questions, 2002.

³⁶Wondji, C. S., R. H. Hunt, et al. (2005). "An integrated genetic and physical map for the malaria vector *Anopheles funestus*." Genetics 171(4): 1779-87.

³⁷Connor, E. E., T. S. Sonstegard, et al. (2004). "An expanded comparative map of bovine chromosome 27 targeting dairy form QTL regions." Anim Genet 35(4): 265-9.

³⁸Zhiming Jiang, Beckman / Coulter A-1928A, MULTIPLEX SNP ANALYSIS: SCREENING FACTOR V R506Q (LEIDEN) MUTATIONS

³⁹<http://www.jax.org/>

⁴⁰Harris, B. S., T. Franz, et al. (1997). "Forebrain overgrowth (fog): a new mutation in the mouse affecting neural tube development." *Teratology* **55**(4): 231-40.

⁴¹Honarpour, N., S. L. Gilbert, et al. (2001). "Apaf-1 deficiency and neural tube closure defects are found in fog mice." *Proc Natl Acad Sci U S A* **98**(17): 9683-7.

⁴²Moreno, S., V. Imbrogliani, et al. (2006). "Apoptosome impairment during development results in activation of an autophagy program in cerebral cortex." *Apoptosis* **11**(9): 1595-602.

⁴³Corvaro M, Cecconi F . APAF1 (Apoptotic protease activating factor 1). *Atlas Genet Cytogenet Oncol Haematol*. September 2004 .

URL : <http://AtlasGeneticsOncology.org/Genes/APAF1ID422.html>